Comment on "Generalized grating equation for virtually imaged phased-array spectral dispersers"

Daniel J. Gauthier

Department of Physics, Duke University, P.O. Box 90305, Durham, North Carolina 27708, USA (gauthier@phy.duke.edu)

Received 9 August 2012; accepted 24 August 2012;
posted 1 November 2012 (Doc. ID 174059); published 29 November 2012

I correct an error made by Vega *et al.* [Appl. Opt. **42**, 4152 (2003)], who derived the spectral dispersion properties of a virtually imaged phased-array etalon using a ray-based, multibounce interference analysis. I demonstrate that the corrected dispersion law is in agreement with the results obtained by paraxial wave theory [Xiao *et al.*, IEEE J. Quantum Electron. **40**, 420 (2004)]. © 2012 Optical Society of America

OCIS codes: 230.0230, 050.2230.

The virtually imaged phase-array (VIPA) spectral disperser is a type of plane-parallel Fabry–Perot etalon in which the reflective coating on the entrance face is removed along a rectangular stripe, often replaced by an antireflection coating. In typical applications, a cylindrical lens focuses the incident light through this transparent window, as shown in Fig. 1. The transmission efficiency of the device approaches 100% when the reflectivity of the entrance face, other than the transparent window, is equal to one and for optimum alignment, which greatly exceeds the efficiency of standard (nonwindowed) Fabry–Perot etalons [1–4].

More recently, Shirasaki [5,6] reinvented the windowed Fabry–Perot, coined the term VIPA, and discussed its application in demultiplexing spectral channels and compensating dispersion in dense wavelength division multiplexing optical telecommunication systems. Over the last decade, Weiner and collaborators have greatly extended this previous work and have used the VIPA in several applications, such as ultrafast optical pulse shaping, arbitrary optical waveform generation, optical telecommunication, and microwave photonics (see [7] for a general review). Recent applications include molecular spectroscopy [8], single-shot measurement of arbitrary nanosecond laser pulses [9], and line-by-line pulse shaping of optical frequency combs [10].

For all of these applications, it is important to have an accurate model for the spectral dispersion of the VIPA. Toward this end, Vega *et al.* [11] derived the VIPA spectral dispersion using a ray-based, multibounce interference analysis [see the geometry in Fig. 2(a)]. Here, a ray incident at angle θ_i with respect to the VIPA normal undergoes multiple bounces through the etalon, where I assume the etalon interior medium and surround space is vacuum for simplicity. They assume that the rays exiting the device propagate at an angle θ_λ with respect to the incoming ray. By considering the phase change from paths $A\bar{B}C$ and $\bar{A}D$, they derive the resonance condition of the etalon

$$2kL\left[\frac{1}{\cos(\theta_i)} - \tan(\theta_i)\sin(\theta_\lambda)\right] = 2m\pi, \qquad (1)$$

where the wavevector magnitude is given by $k = 2\pi/\lambda$, λ is the wavelength of the incident plane wave associated with the ray, and L is the etalon thickness. Under conditions when $\theta_\lambda \ll 1$, Eq. (1) can be expanded to second order in θ_λ to obtain an approximate dispersion relation [12]

$$2kL\left[\cos(\theta_i) - \sin(\theta_i)\theta_\lambda + \frac{1}{2}\tan(\theta_i)\sin(\theta_i)\theta_\lambda^2\right] = 2m\pi. \qquad (2)$$

1559-128X/12/348184-03$15.00/0
© 2012 Optical Society of America

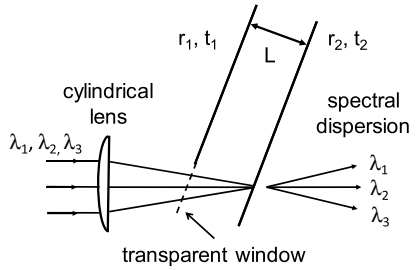

Fig. 1. VIPA spectral disperser. A collimated multiwavelength input beam is focused through the transparent window of the etalon input face and onto the etalon output face with a cylindrical lens. Interference within the etalon causes each wavelength to propagate at different directions with high efficiency. The amplitude reflection and transmission coefficients for the input (output) faces are denoted by r_1, t_1 (r_2, t_2). Typically, $r_1 \sim 1$. The interior of the etalon and the surrounding medium are assumed to be air for simplicity.

Soon thereafter, Xiao *et al.* [12] used a paraxial wave theory to derive the VIPA dispersion law. Here, they considered a Gaussian beam focused by a cylindrical lens on the exit face of the VIPA. The etalon creates an infinite number of virtual images of the Gaussian beam waist, which are displaced both along and transverse to the optical axis. They propagate these images through a lens to a Fourier-transform plane using Fresnel diffraction theory, which allows them to determine the spectral dispersion. To second order in θ_λ, they find the dispersion relation is given by

$$2kL\left[\cos(\theta_i) - \sin(\theta_i)\theta_\lambda - \frac{1}{2}\cos(\theta_i)\theta_\lambda^2\right] = 2m\pi. \quad (3)$$

The third terms in Eqs. (2) and (3) are quite different, which is most pronounced when θ_i is small. Experiments conducted by Xiao *et al.* [12] in this regime confirm the accuracy of Eq. (3) and disprove Eq. (2). It is important to resolve this difference between the approaches because each has advantages in understanding the properties of a VIPA.

I find that there is a fundamental error in the analysis of Vega *et al.* associated with the angle of the rays exiting the VIPA, which is the source of the disagreement between the analysis methods. Because the exit face of the etalon has no prismatic power, a ray passing through the exit face cannot be refracted, contrary to the assumption of Vega *et al.* [see Fig. 2(a)]; that is, only $\theta_\lambda = 0$ is allowed physically. In this case, the dispersion relation is simply given by the standard result for a Fabry–Perot etalon [4]

$$2kL[\cos(\theta_i)] = 2m\pi. \quad (4)$$

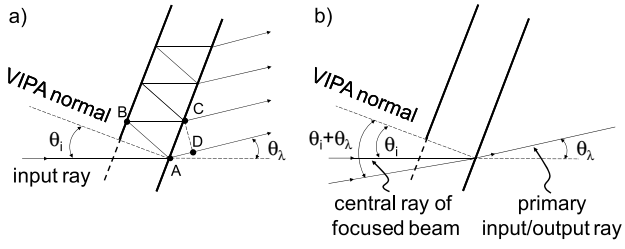

Fig. 2. Ray paths used to determine the VIPA resonances. (a) Geometry used by Vega *et al.* in the ray-based analysis of the VIPA spectral dispersion. (b) Corrected geometry indicating the direction of the central ray of the focused beam (angle θ_i) and for the primary input/output ray in the beam (angle $\theta_i + \theta_\lambda$). The primary ray is not refracted as it is transmitted through the VIPA output face.

As discussed above, an incident beam is focused into the VIPA and so has a spread of angles. Consistent with the approach of Xiao *et al.*, I denote θ_i as the central ray of the focused beam and $\theta_i + \theta_\lambda$ as a ray elsewhere within the focused beam, denoted as the "primary" input/output ray and depicted in Fig. 2(b). The etalon selectively transmits primary rays within the focused beam that satisfy the etalon resonance condition; the input angle of these primary rays is equal to the output angle as shown in the figure. Inserting this definition for the primary-ray angle into Eq. (4) and expanding to second order in θ_λ, I find the approximate dispersion relation

$$2kL\left[\cos(\theta_i) - \sin(\theta_i)\theta_\lambda - \frac{1}{2}\cos(\theta_i)\theta_\lambda^2\right] = 2m\pi, \quad (5)$$

which is identical to the dispersion relation predicted by the paraxial wave theory [Eq. (3)], verified by experiments, and is consistent with Goosman's ray-based analysis [4].

My result demonstrates that both ray-based and wave-theory analysis methods work equally well in understanding the spectral dispersion properties of VIPAs, so that either technique can be used to design optical systems containing these devices.

I gratefully acknowledge discussions of this work with Yunhui Zhu and Hannah Guilbert and the financial support of the DARPA InPho program and the U.S. Army Research Office MURI award W911NF0910406.

References

1. C. Dufour, "Use of the Fabry–Perot interferometer for the study of feeble satellites," Rev. Opt. **24**, 11–18 (1945).
2. C. F. McMillan, N. L. Parker, and D. R. Goosman, "Efficiency enhancements for Fabry–Perots used in velocimetry," Appl. Opt. **28**, 826–827 (1989).
3. C. McMillan and L. Steinmetz, "Striped Fabry–Perots: improved efficiency for velocimetry," Proc. SPIE **1346**, 113–120 (1991).
4. D. R. Goosman, "Formulas for Fabry–Perot velocimeter performance using both stripe and multifrequency techniques," Appl. Opt. **30**, 3907–3923 (1991).
5. M. Shirasaki, "Large angular dispersion by a virtually imaged phased array and its application to a wavelength demultiplexer," Opt. Lett. **21**, 366–368 (1996).
6. M. Shirasaki, "Virtually imaged phased array (VIPA) having air between reflective surfaces," U.S. patent 5,969,866 (19 October 1999).
7. A. M. Weiner, "Ultrafast optical pulse shaping: A tutorial review," Opt. Commun. **284**, 3669–3692 (2011).
8. S. A. Diddams, L. Hollberg, and V. Mbele, "Molecular fingerprinting with the resolved modes of a femtosecond laser frequency comb," Nature **445**, 627–630 (2007).

9. P. Bowlan and R. Trebino, "Complete single-shot measurement of arbitrary nanosecond laser pulses in time," Opt. Express **19**, 1367–1377 (2011).
10. J. T. Willits, A. M. Weiner, and S. T. Cundiff, "Line-by-line pulse shaping with spectral resolution below 890 MHz," Opt. Express **20**, 3110–3117 (2012).
11. A. Vega, A. M. Weiner, and C. Lin, "Generalized grating equation for virtually-imaged phased-array spectral dispersers," Appl. Opt. **42**, 4152–4155 (2003).
12. S. Xiao, A. M. Weiner, and C. Lin, "A dispersion law for virtually imaged phased-array spectral dispersers based on paraxial wave theory," IEEE J. Quantum Electron. **40**, 420–426 (2004).